Available online at www.sciencedirect.com
SCIENCE DIRECT®
Combustion and Flame 144 (2006) 349–359
Combustion and Flame
www.elsevier.com/locate/combustflame

Comparison of burning characteristics of live and dead chaparral fuels ☆

Lulu Sun [a,*], Xiangyang Zhou [a], Shankar Mahalingam [a], David R. Weise [b]

[a] *Department of Mechanical Engineering, University of California, Riverside, CA 92521, USA*
[b] *Forest Fire Laboratory, Pacific Southwest Research Station, USDA Forest Service, 4955 Canyon Crest Drive, Riverside, CA 92507, USA*

Received 22 December 2004; received in revised form 10 July 2005; accepted 10 August 2005

Available online 14 October 2005

Abstract

Wildfire spread in living vegetation, such as chaparral in southern California, often causes significant damage to infrastructure and ecosystems. The effects of physical characteristics of fuels and fuel beds on live fuel burning and whether live fuels differ fundamentally from dead woody fuels in their burning characteristics are not well understood. Toward this end, three common chaparral fuels prevalent in southern California, chamise, manzanita, and ceanothus, were investigated by burning them in a cylindrical container. The observed fire behavior included mass loss rate, flame height, and temperature structure above the burning fuel bed. By using successive images of the temperature field, a recently developed thermal particle image velocity (TPIV) algorithm was applied to estimate flow velocities in the vicinity of the flame. A linear regression fit was used to explain the observed time difference between when maximum flame height and maximum mass loss rate occur, as a function of fuel moisture content. Two different methods were used to extract power laws for flame heights of live and dead fuels. It was observed that the parameters defined in the well-known two-fifths power law for flame height as a function of heat release rate were inadequate for live fuels. As the moisture content increases, the heat release rate in the power law needs to be calculated at the time when the maximum flame height is achieved, as opposed to the maximum mass loss rate. Dimensionless parameters were used to express local temperature and velocity structure of live and dead chaparral fuels in the form of a Gaussian profile over different regimes in a fire plume.

Keywords: Chaparral; Mass loss rate; Flame height; Infrared

1. Introduction

Chaparral is a hardy, fire-prone plant community characterized by evergreen sclerophyll shrubs such as chamise (*Adenostoma fasciculatum*), manzanita (*Arctostaphylos glandulosa*), and hoaryleaf ceanothus (*Ceanothus crassifolius*). Often, two or more species are found interspersed with other shrubs (Fig. 1a). Manzanita and ceanothus are species with leaves that

☆ The U.S. Government's right to retain a nonexclusive royalty-free license in and to the copyright covering this paper, for governmental purposes, is acknowledged.

* Corresponding author.
E-mail address: lsun@engr.ucr.edu (L. Sun).

0010-2180/$ – see front matter © 2005 The Combustion Institute. Published by Elsevier Inc. All rights reserved.
doi:10.1016/j.combustflame.2005.08.008

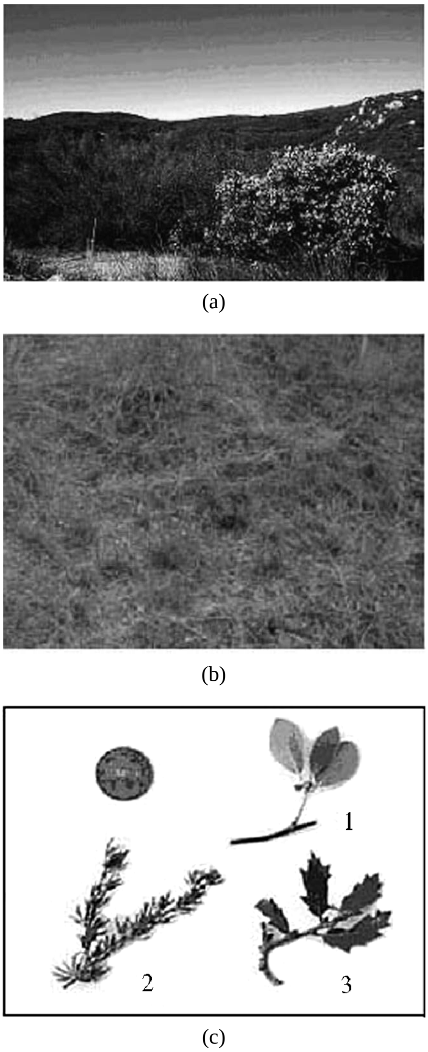

Fig. 1. (a) Chaparral is a mixture of several different species of shrubs that grows in the Mediterranean climate of California. (b) Litter and dead grass. (c) Foliage and fine branch samples of three chaparral species used in the fire plume experiment: (1) manzanita (*Arctostaphylos parryana*), (2) chamise (*Adenostoma fasciculatum*), and (3) hoaryleaf ceanothus (*Ceanothus crassifolius*). Coin diameter is 1.9 cm.

are generally ovoid in shape; however, manzanita leaves are thicker than those of ceanothus. Chamise shrubs range in height from 1 to 3 m with leaves that are linear in shape (Fig. 1c). Fuel depths observed in chaparral crowns (area occupied by branches and foliage) range from 30 to >120 cm, and the crowns tend to be fairly porous (low packing ratio). Surface fuels such as litter and dead grass are often sparse (Fig. 1b). Fire spread in chaparral often occurs in the crowns leading some to describe fires in this vegetation type as a crown fire.

Fire burns large areas in living chaparral fuels in southern California annually [1]. The ability to predict fire spread in these fuels is limited by the fact that current fire-spread models were designed primarily for dead fuels and only a limited set of experimental data exist for testing models. This problem has been recognized for 60 years [2,3]. Recently, in Europe and Australia, modeling of fire spread in various live fuels has occurred [4–8], and in the United States, there are limited empirical and modeling tools to predict fire spread in live fuels [9–19].

Rothermel's [20] semiempirical fire-spread formulation forms the basis of current computer-based operational models utilized in the United States, including BEHAVE [21] and FARSITE [22]. It is applicable for fuel beds dominated by dead fuel. However, fuel moisture has long been recognized as having a major influence on the ignition, development, and spread of fires [23]. The moisture content of a fuel is the mass of water in that fuel, expressed as a percentage of the oven-dry weight of that fuel. Thus, if the fuel were totally dry, then the fuel moisture content would be zero. That being said, when a fuel has less than 30% moisture content, it is basically a dead fuel and is treated as such. In the case of living fuels, moisture content ranges from 30 to around 300%. The moisture content of dead fuels responds quickly to changes in relative humidity and temperature, whereas the moisture content of live fuels depends largely on physiological activity within the vegetation and soil moisture availability. One expects a fire would behave differently in live and dead fuels. But details of the combustion processes unique to living vegetation are unknown and may explain the dynamic fire behavior observed in these fuels. Fire spreads successfully in live chaparral fuels at higher fuel moistures than most of the experimental data used to develop the Rothermel model. Under the influence of strong Santa Ana winds, nearly 304,000 ha were burned in southern California during October 21–November 4, 2003 [24]. Fuel moisture content in live chaparral was around 60–85% at that time.

Given that current operational models do not adequately model fire spread in chaparral fuels and that data describing burning characteristics of chaparral fuels are limited, we have embarked upon an experimental effort to determine burning characteristics of live and dead chaparral fuels. In this paper, we focus on a simplified configuration of a fire plume. The fire plume represents a front of a propagating fire and includes all the relevant physical and chemical mechanisms occurring within a spreading flame front. It is basically a buoyant diffusion flame established over a finite mass of fuel in a container and characterized by three distinct regimes: the persistent flame, the intermittent flame, and the buoyant plume [25]. The quantities of fundamental importance in such flames are the mass loss rate of solid fuel, heat release rate, flame height, temperature, and velocity structure. Flame height may be determined from measurements made from video recordings and short-time exposure photographs. Although various definitions of flame height exists, in this paper the definition proposed by Zukoski et al. [26] was utilized. This uses the 50% visible intermittency height as a characteristic flame height, and is defined as the location where the flame resides above and below this threshold, 50% of the time. Because the wavelengths of thermal emissions are in the infrared (IR) range between 3 and 15 µm, and thermal emission is proportional to the fourth power of surface temperature, IR cameras have been used successfully to detect and map temperature fields within wildfires [27–33]. An IR image represents a sheet of data in the x–z plane with the y (depth coordinate) varying over the image. It allows investigation of physical mechanisms involving fire-spread rate through use of image flow analysis. We recently developed a thermal particle image velocity (TPIV) algorithm for nonintrusively estimating flow velocities within the vicinity of a flame through IR camera [34]. TPIV follows the method established in gradient-based algorithms [28] and uses the basic idea of the PIV technique. By tracing "thermal particles" across successive IR images, the TPIV algorithm can provide an easier and more convenient instantaneous velocity measurement area than either a single-point velocity measurement [35,36] or area velocity measurement such as PIV. In TPIV, the seed particles are represented by "thermal particles," which are assumed to be virtual particles that correspond to pixels of temperature values resolved in IR images. The signal from a thermal particle is the irradiance measured by an IR thermal camera. It is assumed that thermal particles rotate and translate, behaving like fluid particles, and their temperatures are conserved over the short time step between images that is required for analysis. For details of the technique, see Zhou et al. [34].

In Section 2, the experimental procedure and data collection methods are described. The measured quantities include mass of solid fuel, flame height, temperature, and estimates of velocity structure, all as functions of time over which the fuel sample is completely burnt. The main experimental results are summarized and discussed in Section 3. Conclusions are given in Section 4.

2. Experimental details

The experiments were carried out in the burn facility located at the United States Department of Agriculture Forest Service (USDAFS) Forest Fire Laboratory in Riverside, California. This facility is a metal building 13 × 13 m with 6.1-m walls and a vented, peaked roof that is 7.6 m above the concrete floor. The air is unconditioned and introduced at ground level to provide a pressure differential to force smoke through the roof vent. The air flow is high-volume and sufficiently low-velocity not disturb the experiment.

2.1. Fuel collection

2.1.1. Live chaparral fuels

Fuel samples were collected from living chaparral growing at an elevation 1160 m in an area 50 km east of Riverside, CA (Fig. 1a) in spring (April) and fall (September–October). Spring represents the period of growth following winter rains and fall represents the dormant period during which plants minimize moisture loss. Foliage and branches <0.64 cm from chamise, manzanita, and hoaryleaf ceanothus plants comprised the fuels (Fig. 1c). Plant material was collected in the morning to minimize moisture loss through transpiration. Visually identified dead wood and foliage were removed to the extent possible. The fuels were then bagged and transported to the burn facility at the Forest Fire Laboratory and were burned on the day of collection to minimize moisture loss and approximate plant living conditions as much as possible.

2.1.2. Dead chaparral fuels

After the experiments utilizing live chaparral fuels were completed, the leftover fuels remained indoors in the laboratory and dried out for several weeks until the fuel moisture content stayed unchanged. We treated these as dead fuels and burned them.

2.2. Experimental setup

Fig. 2 shows a photograph of our experiment and a schematic of the experimental apparatus. A fuel bed was constructed by uniformly distributing a fixed mass of chaparral in a circular screen container of known diameter. Extraneous vertical strands above the screen surface were then clipped. A paper towel saturated with the isopropyl alcohol was placed below the screen container. The diameter of the paper towel was the same as that of the fuel bed. The amount of alcohol saturated by paper was sufficient to ignite the fuel bed without great perturbation of the fire behavior of the chaparral fuel bed. This quantity was determined by trial and error before the experiment and varied from 5 to 6% of the fuel (wet basis) mass. The entire assembly rested on an electronic scale (8 kg maximum loading, 0.1 g resolution). The fuel mass $m(t)$ was determined by recording the sample mass at

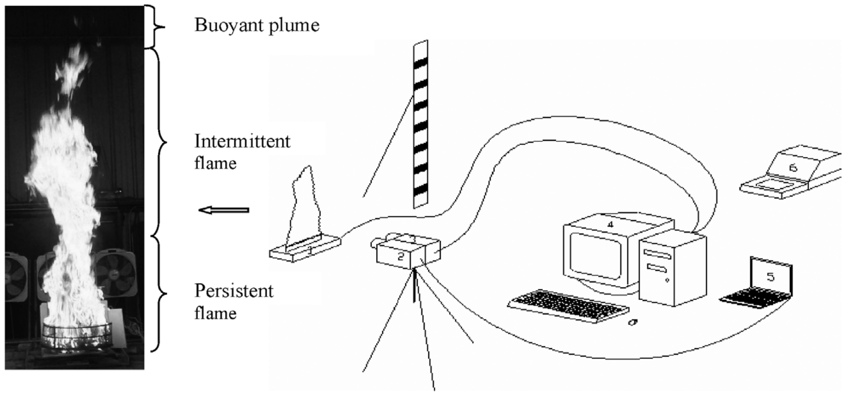

Fig. 2. Experimental apparatus: (1) electronic scale, (2) infrared camera, (3) digital camcorder, (4) computer workstation, (5) IBM laptop, (6) Computrac moisture analyzer.

a frequency of 1 Hz using this electronic scale, and the mass loss rate dm/dt was numerically estimated using central differencing. A Canon-ZR40 digital video camera was used to record the experiment at a frame rate of 30 Hz. The electronic scale and the video camera were connected to a computer data acquisition system via an RS-232 port and Labview (National Instruments Co.) software. The temperature structure of the fire plume was measured by a FLIR ThermaCAM SC500 IR-camera at a frame rate of 60 Hz. ThermaCAM 2000 software was used to obtain 320 × 240 pixel temperature field. Fuel moisture content (oven-dry basis) was determined using a Computrac moisture analyzer immediately prior to burning. Sample dry mass was determined from the measured sample mass and the estimated moisture content.

Chaparral plant moisture content generally follows a sinusoidal annual trend. In our experiment the moisture content was not controlled, but this trend was utilized to vary the effects of live fuel moisture over the course of different seasons in an annual cycle. Three different fuel-bed diameters ($d = 30$, 45, and 60 cm) were constructed and the fuel containers cooled to ambient temperatures between successive experiments. A constant fuel loading (dry mass per unit of fuel bed area) of 2.12 kg/m^2 was used. As the higher fuel height would lead to taller flame height because of the increased fuel loading [37], the fuel bed depth was kept constant and equal to the height of the container (20 cm). Particle density was determined using the "water displacement method." Measurements of the high heat of combustion of live and dead shrub samples using standard oxygen bomb calorimetry methods have been reported [38,39]. Since both the foliage and less than 0.64-cm size class had nearly identical average high heats of combustion, we used an averaged value of 20.89 kJ/g based on their measurements. A low heat of combustion value of 14.71 kJ/g was used, based on the volatiles released during pyrolysis of the shrub fuels and measured using a thermochemical analysis in [40]. Three replications of each diameter for each species studied yielded a series of 81 experimental fire plumes. Fuel and ambient conditions associated with the various tests were recorded and are summarized in Table 1.

3. Results and discussion

Branches and foliages of shrub fuel arranged in circular horizontal containers were burned in the laboratory (Fig. 2). By varying the diameters of the containers and fuel conditions (live or dead), we investigated a range of burning rates.

3.1. Mass loss rate of live and dead chaparral fuels

Due to natural fuel-bed variability and entrainment of environmental air, the bottom of the fuel bed could not be ignited uniformly. The fire started generally from the center and then spread to the edge of the container. This is different from liquid pool fires, where ignition of the entire surface is rapid due to high flame-spread rates. After ignition of the fuel bed, the mass loss rate reached a maximum value. This is illustrated in Fig. 3, in which the mass loss rate (curve fit) of live and dead shrub fuels for container diameter 45 cm is plotted. In all cases, the fuel loading was kept constant at 2.12 kg/m^2, as was indicated in Section 2. Generally the mass loss rate of live shrub fuels is higher than that of dead shrub fuels because of their higher moisture content. Biswell [41] noted that chamise is generally considered to be highly flammable compared to other chaparral species, while ceanothus resists fire well when young. Comparing the time when the maximum mass loss rate of these three dead shrub fuels is attained, we found that

Table 1
Fuel and environmental conditions

Species status		Date mm/dd/yy	Moisture content (%)		Density (kg/m^3)	Relative humidity (%)	Ambient temperature (K)
			Mean	SD[d]			
Live[a]	Chamise	04/21/03	90	6.3	662	45	292
	Manzanita	04/17/03	91	6.6	674	40	284
	Ceanothus	04/25/03	90	6.1	599	50	300
Live[b]	Chamise	09/18/03	53	4.2	662	45	305
Live[c]	Manzanita	10/25/04	79	0.3	674	42	295
	Ceanothus	10/26/04	78	3.3	599	50	295
Dead	Chamise	12/02/03	12	1.5	801	45	292
	Manzanita	12/03/03	9	0.4	639	45	292
	Ceanothus	12/03/03	9	0.7	554	45	292

[a] Shrub fuels collected in April (spring season).
[b] Chamise fuels collected in September (fall season).
[c] Manzanita and ceanothus collected in October (fall season).
[d] Standard deviation.

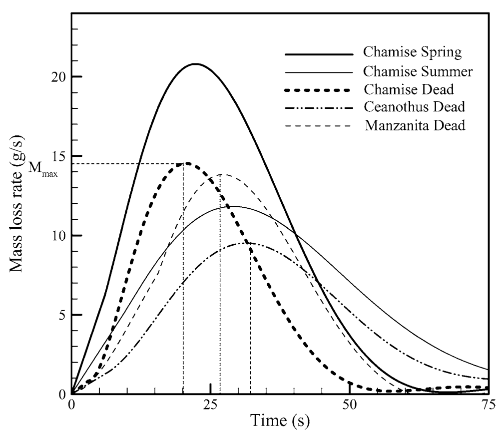

Fig. 3. A comparison of mass loss rate of live and dead chaparral fuels during different seasons (noted in the figure) in an annual cycle.

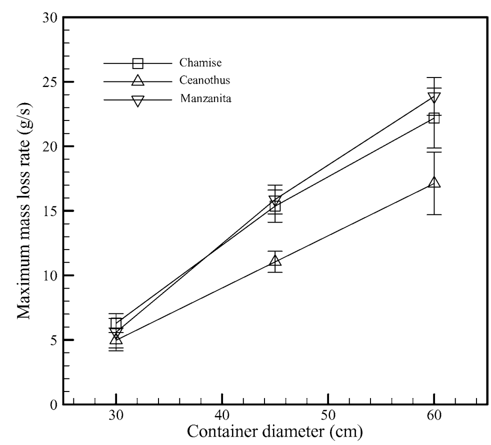

Fig. 4. Maximum mass loss rate versus container diameter of dead chaparral fuels.

chamise reached the maximum mass loss rate faster than manzanita, while ceanothus was slowest. This result is consistent with Biswell conclusion. From Fig. 4 it is seen that the species type weakly affected the maximum mass loss rate and the maximum mass loss rate increased with the container diameter because more fuel mass was involved. Koseki and Yumoto [42] and Chatris et al. [43] conducted large-pool fire experiments (the maximum container diameter reached 6 m) and observed that the maximum mass loss rate increased with container diameter. Chatris et al. mentioned that the maximum mass loss rate would reach a maximum value at a certain diameter, which remains constant for larger diameters. Di Blasi et al. [44] discussed that under low external heat flux, as the moisture content of the fuels increases, moisture evaporation and wood pyrolysis processes occur sequentially [44]. In our experiments the external heat flux used to ignite the fuels is minimized by using the minimum amount of alcohol necessary for ignition; our external heat flux falls into the low-external-heat-flux region. The entire combustion process may be subdivided into three phases. The first phase, corresponding to early times, involved completion of combustion of the ignition source and the moisture loss of shrub fuels. Due to the relatively high moisture content of live shrub fuels in spring and fall seasons, a large amount of white smoke was visible during this phase. The second phase involved mainly ignition and subsequent combustion of pyrolysate gases released from the heated solid surface of shrub fuels. Little carbon was burned. Under control of buoyancy forces, combustion of the pyrolysate formed a fire plume above the fuel bed. The initial ignition time was longer (about 36 s) than that for dead shrub fuels (about 6 s) (see Fig. 5). At the region above the top of the flame, black smoke with flash soot was

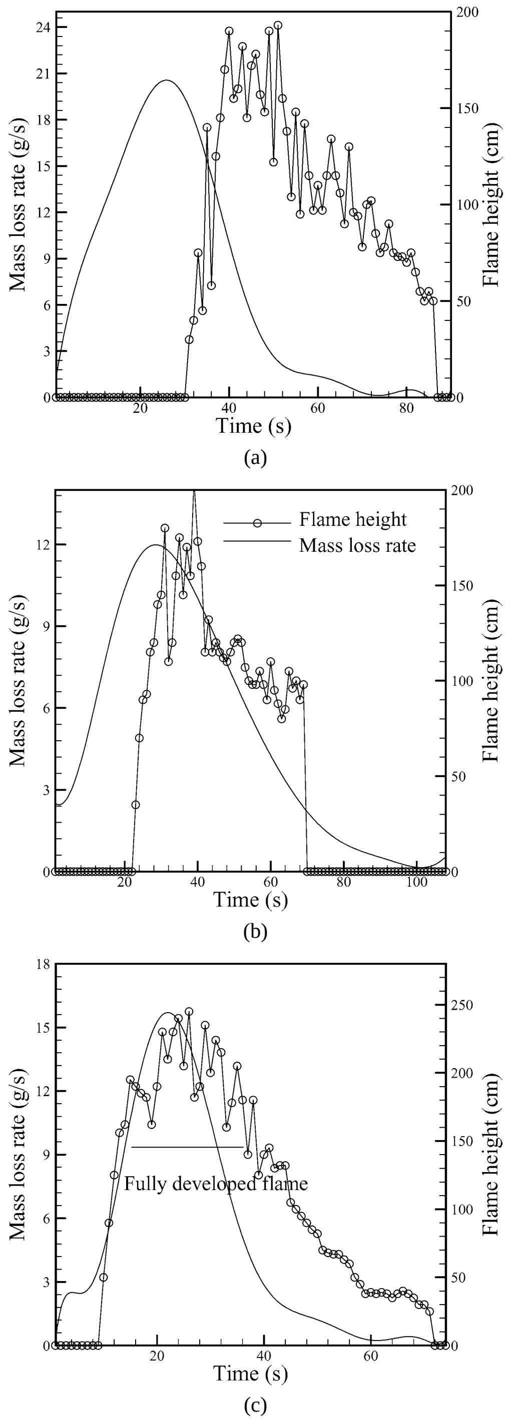

Fig. 5. Time evolutions of mass loss rate and corresponding flame height of live chamise fuels (a) in spring, (b) in fall and (c) dead chamise fuels.

visible. In this paper, the reported fire plume properties such as maximum flame height were averaged over this steady burning period. After the burning of volatile gas, the final burning phase was the combustion of carbonaceous residue at a reduced burning rate. The mass loss rate decreased slowly and finally reached zero. The total combustion process was then completed.

3.2. Flame height of chaparral fuels

A common definition for flame height is that of the visible edge of flame luminescence. Following this rule, we measured flame height Z_{fl} from the visible images. Due to the existence of smoke around the upper part of flame, the uncertainty in measuring flame height was estimated to be ±5%. Fig. 5 shows the mass loss rate and corresponding flame height of live (in spring and fall season) and dead chamise at a sampling rate of 1 Hz over all three phases of the entire combustion process. Several observations can be made from this data set. First, we saw that the flame height was reached maximum a few seconds after ignition. It remained steady from ∼30 s for dead chamise fuels to ∼45 s for live chamise fuels burned in spring. This quasi-steady-state showed that a fully developed flame was reached and we defined the maximum flame height as the moving average value over 4 s during this stage. A video recording rate of 30 images/s was used to display and calculate this value. Second, it is evident that the times at which maximum mass loss rate was realized and maximum value of flame height occurred were distinctly different. This difference in time Δt is defined as $\Delta t = t_{\mathrm{M}} - t_{\mathrm{H}}$, where t_{M} and t_{H} denote the times at which mass loss rate and flame height attain their respective maxima. In Fig. 5a, when live chamise was burned in spring season, the maximum mass loss rate was reached ∼30 s earlier than the maximum flame height; in Fig. 5b when live chamise was burned in fall season, the maximum mass loss rate was reached ∼20 s earlier than the maximum flame height; in Fig. 5c, when dead chamise was burned, the maximum mass loss rate was reached ∼6 s earlier than the maximum flame height. The relationship between moisture content M of shrub fuels and the time shift Δt can be expressed by a linear fit,

$$\Delta t = 0.4(M - 0.4), \quad (1)$$

as illustrated in Fig. 6.

In general, the maximum flame heights of dead shrub fuels were higher than those of live shrub fuels because the flame height depends strongly on the heat release rate of the fire [26]. The heat release rate is simply defined as

$$Q_{\mathrm{f}} = -h(\mathrm{d}m/\mathrm{d}t), \quad (2)$$

where for the low heat of combustion h, as mentioned previously in Section 2, an averaged value of

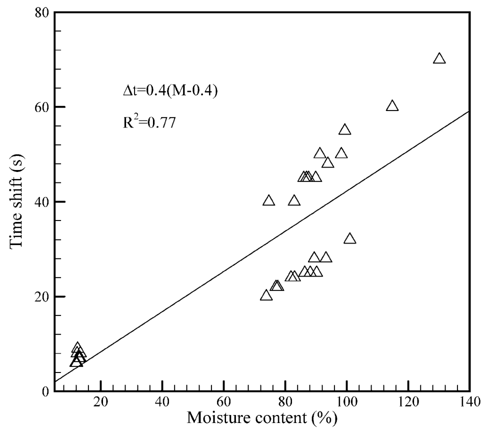

Fig. 6. Time shift versus moisture content of live and dead shrub fuels.

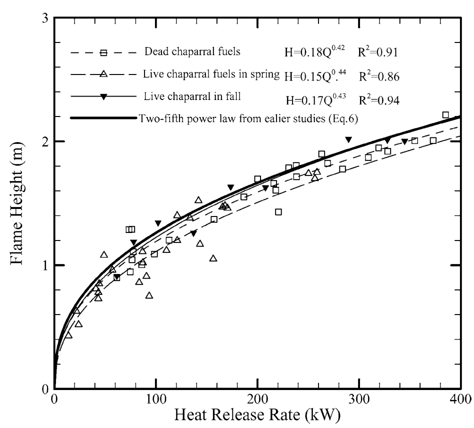

Fig. 7. Maximum flame height versus maximum heat release rate for live and dead chaparral fuels (method 1) and two-fifths power law from earlier studies is also shown for reference.

$h = 14.71$ kJ/g was used. Here we used two different methods to calculate the mass loss rate dm/dt. First it is calculated as the maximum mass loss rate $\dot{M}_{\rm max}$ shown in Fig. 3 (method 1). Using this value, three power laws for flame heights were derived using a linear least-squares fit (also see Fig. 7):

$$H_{\rm l} = 0.17\dot{Q}_{\rm l}^{0.43}, \tag{3}$$

$$H_{\rm d} = 0.18\dot{Q}_{\rm d}^{0.42}, \tag{4}$$

$$H_{\rm h} = 0.15\dot{Q}_{\rm h}^{0.44}. \tag{5}$$

Equation (3) describes maximum flame height $H_{\rm l}$ against maximum heat release rate $\dot{Q}_{\rm l}$ for chaparral fuels burned in fall season. Equation (4) was derived for dead chaparral fuels and Eq. (5) was obtained from chaparral fuels burned in spring season. Earlier theoretical and experimental studies [25,26,45,46], including Dupuy et al.'s [37] study for oven-dried solid

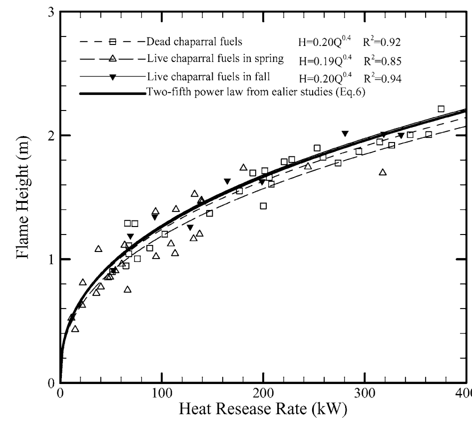

Fig. 8. Maximum flame height versus maximum heat release rate for live and dead chaparral fuels (method 2) and two-fifths power law from earlier studies also is shown for reference.

fuels show a two-fifths power law for maximum flame height ($H_{\rm max}$) and maximum heat release rate ($\dot{Q}_{\rm max}$) in the case of buoyant diffusion flames:

$$H_{\rm max} = 0.2\dot{Q}_{\rm max}^{2/5}. \tag{6}$$

They calculated the maximum heat release rate $\dot{Q}_{\rm max}$ using maximum mass loss rate $\dot{M}_{\rm max}$. Apparently they all show some deviation, especially Eq. (5) for high-moisture-content live fuels. This is understandable because the maximum mass loss rate obtained in spring season is mostly due to vaporization of a large amount of water vapor appearing as white smoke from the foliage and surface layers of branches, and not because of combustion of pyrolysate from the heated solid surface. Hence it is argued that it is inappropriate to use maximum mass loss rate to calculate maximum heat release rate for live fuels.

As an alternative, we considered using the mean value of the mass loss rate corresponding to the same time period when the maximum flame height was reached to calculate the mass loss rate (method 2). We hypothesized that the maximum heat release rate due to combustion and maximum flame height occurred at the same time. Using this method, three different power laws given by Eqs. (7)–(9) were extracted from the data to express the relationship between heat release rate and flame height for live fuels burned in fall and spring season and dead shrub fuels, respectively (also see Fig. 8). These correlations are given by

$$H_{\rm L} = 0.20\dot{Q}_{\rm L}^{0.40}, \tag{7}$$

$$H_{\rm H} = 0.19\dot{Q}_{\rm H}^{0.40}, \tag{8}$$

$$H_{\rm D} = 0.20\dot{Q}_{\rm D}^{0.40}, \tag{9}$$

where Eq. (7) describes the maximum flame height $H_{\rm L}$ and corresponding heat release rate $\dot{Q}_{\rm L}$ for chaparral fuels burned in fall season, Eq. (8) was obtained for chaparral fuels burned in spring season, and Eq. (9) was derived for dead chaparral fuels. Also shown in the figure is the two-fifths power law (Eq. (6)) from earlier studies for reference. It appears that the two-fifths power law is now reasonable for live and dead fuels. Our results demonstrate that the parameters defined in the two-fifths power law only fit for dead or dry fuels. For high-moisture live fuels, we need to use the heat release rate corresponding to the maximum flame height to derive the power law. Then the simple power law to fit the entire set of our data can be written as

$$H = 0.2\dot{Q}^{2/5}. \tag{10}$$

In the fire literature a dimensionless heat release rate term, introduced in the 1970s by Zukoski [47] and others, is the square root of a Froude number (U^2/gD), where U is the velocity of the gases, D is the diameter of the container, and g is the acceleration due to gravity used to classify fire types and correlate aspects of fire behavior, such as flame height. Assuming fuel density ρ, and heat of combustion of the fuel vapor of ΔH_c, the initial velocity of the fuel vapors can be expressed as

$$U = \frac{\dot{Q}}{\Delta H_c \rho (\pi D^2/4)}. \tag{11}$$

Then the dimensionless heat release rate can be given as

$$Q^* = \frac{\dot{Q}}{\rho_\infty T_\infty c_{p\infty} D^2 \sqrt{gD}}, \tag{12}$$

where $c_{p\infty}$, T_∞, and ρ_∞ are specific heat, temperature, and density of ambient air. The results of Zukoski [26] suggest that Q^* is one of the most important parameters in controlling the geometry of fire plumes. The dimensionless flame height is scaled as Z_{fl}/D. Using the second method to calculate the heat release rate, the dimensionless flame heights are shown in Fig. 9 in the form of a scatterplot of Z_{fl}/D versus Q^*. For comparison, the dimensionless result of Zukoski obtained for gas fuels [26] and a unified analysis for fire plumes over a wide range of Q^* [48] are also plotted in this figure. In the figure the dimensionless flame height Z_{fl}/D increases with Q^*. The dimensionless flame height in the case of chaparral fuels is nearly consistent with the Zukoski [26] correlation for gas fuels but is underpredicted by the unified analysis of Zukoski [48]. The dimensionless results agree with the dimensional power-law results.

3.3. Temperature structure

Assuming a Gaussian profile for time-averaged temperature difference, $\Delta T = T(r,z) - T_\infty$, as a function of the radial coordinate r, the normalized temperature can be expressed as

$$\frac{T(r,z) - T_\infty}{T_m(z) - T_\infty} = \exp\left[-\alpha (r/R_t)^2\right], \tag{13}$$

where $T(r,z)$ is the time-averaged temperature at a specific radial location and height z above the bottom of the fuel bed, $T_m(z)$ is the maximum temperature at that height, and T_∞ is the environmental temperature. The quantity R_t is the Gaussian half-width for temperature profiles at a specific height. The quality α is a parameter that can be estimated from temperature profiles. The time-averaged temperature value was defined as a moving average value over 4 s in the fully developed flame region. Fig. 10 shows normalized temperature profiles of chaparral fuels in the intermittent region above the surface of the container. The estimated parameters α in this region for dead and live chaparral fuels are shown in the figure.

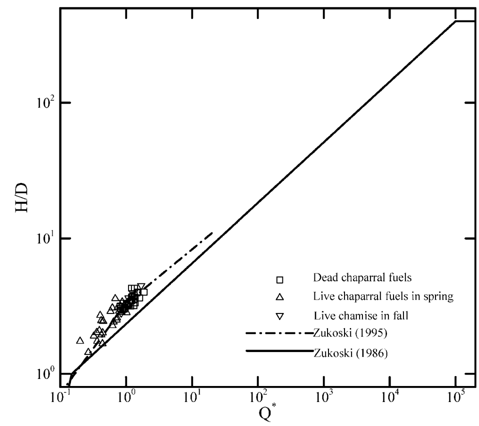

Fig. 9. Normalized flame heights of three live and dead shrub fuels are scattered versus normalized flame heat release rate (method 2). The result from Zukoski is also illustrated as a solid line.

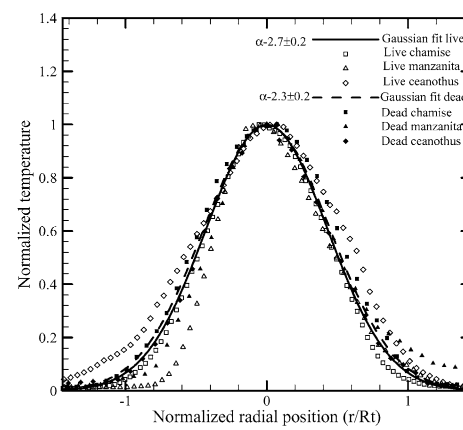

Fig. 10. Radial profiles of normalized excess temperature in the persistent flame region.

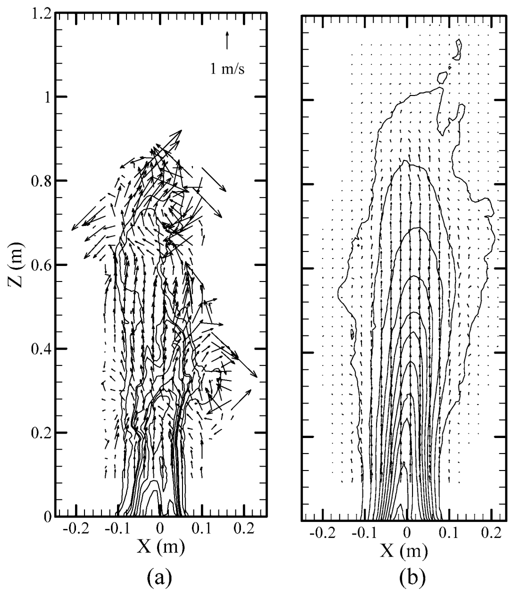

Fig. 11. (a) Instantaneous and (b) time-averaged velocity fields of live chamise in fall season.

3.4. Velocity structure

Using the digital temperature images captured by the IR camera, the velocity field of the fire plume was estimated via the TPIV algorithm [34]. Because each IR thermal image is averaged over a significant depth into the flame front, the estimated velocity components are representative for similar depth. Apparent motions in the image may contain motions into or out of the image, whereas we estimate only those that project onto the two-dimensional distorted sheet.

To estimate the velocity field, the TPIV algorithm with a patch size of 13 × 13 pixels was applied to a sequence of 240 temperature images, which corresponds to a time period of 4.0 s. For container diameter 45 cm, an instantaneous velocity vector field and time-averaged velocity vector field of live chamise fuels burned in fall are shown in Figs. 11a and 11b, respectively. The vector illustrates the magnitude and the direction of the velocity. Although the velocity field shown in Fig. 11a is estimated over three images, because the time period is short (0.03 s), the velocity field is still assumed to be instantaneous. The time-averaged velocity is calculated over 4.0 s. Because of the turbulent nature of the flow, the instantaneous velocities reveal large scale rotating vortices and large fluctuations from the time-averaged values. There is an accelerating central core in the fire plume and strong rotation at the center and the edge of the plume. This is consistent with the vortex observed visually during the experiment. It is known that the fire vortex leads to strong radial inflow of ambient air into the core of the fire. The estimated velocity field is useful to describe the small temporal and spatial scales involved in the fire vortices that help to determine fire spread. The estimated peak value of instantaneous vertical velocity is about 2.8 m/s and the averaged value is 0.7 m/s.

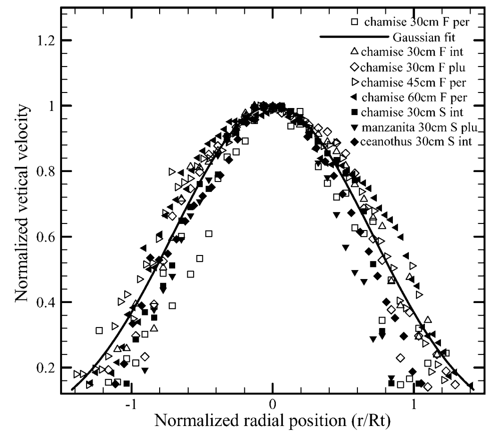

Fig. 12. Radial profile of normalized vertical velocity versus normalized radial position.

With the increase of container diameter from 30 to 45 to 60 cm, analysis of successive velocity data suggests that the puffing frequency decreases from 2.64 to 2.42 to 2.16 Hz, respectively, which is essentially in agreement with observations made by Zukoski [26] and Pagni [49].

Similarly to temperature profiles, the shape of time-averaged vertical velocity profile is also close to Gaussian. Zukoski [26] assumed that the normalized velocity is given by

$$\frac{w}{w_{\mathrm{m}}} = \exp\left[-\left(\frac{r}{R_v}\right)^2\right], \tag{14}$$

where w denotes an averaged flame velocity at a radial location, w_{m} is the maximum averaged velocity at that downstream location, and R_v is the Gaussian half-width for velocity profiles. Using the velocity data estimated from the TPIV algorithm, Fig. 12 illustrates the plot of the normalized vertical velocity versus the normalized radial position for chaparral fuels. It can be noticed that all chaparral fuels can be represented by one fitted Gaussian profile. Validation of the TPIV algorithm was done by comparing the results from this simple fast method to an accurate method of measurement, namely particle image velocimetry [50].

4. Conclusions

Chamise (*Adenostoma fasciculatum*), manzanita (*Arctostaphylos glandulosa*), and hoaryleaf ceanothus

(*Ceanothus crassifolius*) are among the most hazardous shrub fuels that grow in the mountains of southern California and throughout the coastal ranges. This paper focuses on a comparison of overall burning characteristics of these three live and dead shrub fuels by investigating the mass loss rate, flame height, temperature, and velocity structure over a fire plume. In all cases, constant fuel loading was utilized. Noting that the time when the maximum mass loss rate is attained is the lowest, it is concluded that chamise is the most flammable of the three species examined in this paper. An empirical relationship was found to fit moisture content of shrub fuels and time shift from maximum mass loss rate to maximum flame height. It was observed that flame height increases with heat release rate. Two different methods were used to extract scaling laws to describe a relationship between flame height and heat release rate for both live and dead chaparral fuels. In method one, maximum mass loss rate was used to obtain a power law for maximum flame height and maximum heat release rate. In the second method, the mean value of the mass loss rate at the time when the maximum flame height is reached was used to compute heat release rate and develop a power law for live and dead shrub fuels. The calculation results indicate that the heat release rate defined in the two-fifth power law is inadequate for calculating live fuels. As the moisture content increases, the heat release rate calculated at the time when the maximum flame height is attained is more consistent with the two-fifths power law. Using dimensionless parameters, a Gaussian fit can be used to express the local radial temperature profile of chaparral fire plumes. Velocity results based on a thermal particle image velocimetry method appear reasonable, and a Gaussian profile fits the data well. The current results show that the burning characteristics of live chaparral fuels in a fire plume are different from dead chaparral fuels when we consider mass loss rate, flame height, and heat release rate. Using dimensionless parameters, simple explicit relationships were established to describe the chaparral fire plume. These results will be useful for the study of wildfire spread in live chaparral fuels.

Acknowledgments

The funding source for this research is the USDA/USDI National Fire Plan administered through Research Joint Venture Agreement 01-JV-11272166-135 with the Forest Fire Laboratory, Pacific Southwest Research Station, USDA Forest Service, Riverside, CA. The instrument names in this paper are provided for informational purposes only and do not constitute endorsement by the U.S. Department of Agriculture. We appreciate the efforts of Joey Chong and David Kisor in collecting the fuels, building the fuel beds, and assisting in performing the experimental burns.

References

[1] C. Philpot, in: Proc. Symposium Environmental Consequences Fire and Fuel Management in Mediterranean Ecosystems, 1977, pp. 12–16.
[2] C.C. Buck, H.D. Bruce, C.A. Abell, W.L. Fons, A Forest Fire Protection Problem Analysis for California, RS-Cal Research Program, 1941, pp. 1–142.
[3] R.M. Nelson, D. Bruce, J. Forestry 56 (1958) 399–403.
[4] J.B. Marsden-Smedley, W.R. Catchpole, A. Pyrke, Int. J. Wildland Fire 10 (2) (2001) 255–262.
[5] P.A.M. Fernandes, Forest Ecol. Management 144 (2001) 67–74.
[6] E. Bilgili, B. Saglam, Forest Ecol. Management 184 (2003) 201–207.
[7] M. De Luis, M.J. Baeza, J. Raventos, J.C. Gonzalez-Hildalgo, Int. J. Wildland Fire 13 (2004) 79–87.
[8] D. Morvan, J.L. Dupuy, Combust. Flame 138 (2004) 199–210.
[9] F.A. Albini, Proc. Combust. Inst. 11 (1967) 553–560.
[10] R.C. Rothermel, C.W. Philpot, J. Forestry 71 (1973) 640–643.
[11] F.A. Albini, E.B. Anderson, Predicting Fire Behavior in U.S. Mediterranean Ecosystems, USDA General Technical Report PSW-58, 1982.
[12] J.D. Cohen, Estimating Fire Behavior with FIRECAST: User's Manual, USDA General Technical Report PSW-90, 1986.
[13] F.A. Albini, B.J. Stocks, Combust. Sci. Technol. 48 (1986) 65–76.
[14] B.W. Butler, M.A. Finney, P.L. Andrews, F.A. Albini, Can. J. Forest Res. 34 (2004) 1588–1599.
[15] L.R. Green, Burning by Prescription in Chaparral, USDA General Technical Report PSW-51, 1981.
[16] S. Raybould, T. Roberts, USDA Forest Service Fire Manage. Notes 44 (1983) 7–10.
[17] D. Campbell, Wildland Fire Specialists (1995) 129.
[18] D.R. Wise, X. Zhou, L. Sun, S. Mahalingam, Int. J. Wildland Fire 14 (2005) 99–106.
[19] X. Zhou, D.R. Wise, S. Mahalingam, Proc. Combust. Inst. 30 (2005) 2287–2294.
[20] R.C. Rothermel, USDA Forest Service Research Paper INT-115, 1972.
[21] P.L. Andrews, BEHAVE Fire Behavior Prediction and Fuel Modeling System, USDA Forest Service General Technical Report INT-194, 1986.
[22] M.A. Finney, FARSITE: A Fire Area Simulator for Managers, USDA Forest Service General Technical Report ST-X-3, 1995.
[23] L.F. Hawley, J. Forestry 24 (1926) 756–763.
[24] W. Campbell, Governor's Blue Ribbon Fire Commission Report to the Governor, 2004.
[25] B.J. McCaffrey, Purely Buoyant Diffusion Flames: Some Experimental Results, National Bureau of Standards Report NBSIR 79-1910, 1979.

[26] E.E. Zukoski, in: G. Cox (Ed.), Combustion Fundamentals of Fire, Academic Press, London, 1995, p. 101.
[27] J. Coen, S. Mahalingam, J.W. Daily, J. Appl. Meteor. 43 (2004) 1241–1259.
[28] T.L. Clark, L. Radke, J. Coen, D. Middleton, J. Appl. Meteor. 38 (1999) 1401–1420.
[29] P.J. Riggan, R.G. Tissell, R.N. Lockwood, J.A. Brass, A.P. Pereira, H.S. Miranda, A.C. Miranda, T. Campos, R. Higgins, Ecol. Appl. 14 (3) (2004) 855–872.
[30] P.J. Riggan, J.W. Hoffmann, J.A. Brass, in: Proceedings of the 2000 IEEE Aerospace Conference, vol. 3, 2000, pp. 173–179.
[31] P.J. Riggan, J.W. Hoffman, in: Proceedings of the 1999 IEEE Aerospace Conference, vol. 3, 1999, pp. 443–449.
[32] P.J. Riggan, R.G. Tissell, J.W. Hoffman, in: Proceedings of the 2003 IEEE Aerospace Conference, vol. 4, 2003, pp. 1863–1872.
[33] P.J. Riggan, J.W. Hoffman, in: Proceedings of the 2003 IEEE Aerospace Conference, vol. 4, 2003, pp. 1843–1854.
[34] X. Zhou, L. Sun, D.R. Weise, S. Mahalingam, Combust. Sci. Technol. 175 (2003) 1293–1316.
[35] B.J. McCaffrey, G. Heskestad, Combust. Flame 26 (1976) 125–127.
[36] G. Cox, Combust. Flame 28 (1977) 155–163.
[37] J.L. Dupuy, J. Marechal, D. Morvan, Combust. Flame 135 (2003) 65–76.
[38] C.M. Countryman, Physical Characteristics of Some Northern California Brush Fuels, USDA General Technical Report PSW-61, 1982.
[39] C.M. Countryman, C.W. Philpot, Physical Characteristics of Chamise as a Wildland Fuel, USDA Forest Service Research Paper PSW-66, 1970.
[40] F.A. Albini, Thermochemical Properties of Flame Gases from Fine Wildland Fuels, USDA Forest Service Research Paper INT-243, 1980.
[41] H.H. Biswell, in: Fire and Ecosystems, Academic Press, New York, 1974, pp. 321–364.
[42] H. Koseki, T. Yumoto, Fire Technol. 2 (1988).
[43] J.M. Chatris, J. Wuintela, J. Folch, E. Planas, J. Arnaldos, J. Casal, Combust. Flame 126 (2001) 1373–1383.
[44] C. Di Blasi, E.G. Hernadez, A. Santoro, Ind. Eng. Chem. Res. 39 (2000) 873–882.
[45] G. Cox, R. Chitty, Combust. Flame 39 (1980) 191–209.
[46] F.R. Steward, Combust. Sci. Technol. 2 (1970) 203.
[47] E.E. Zukoski, Convective Flows Associated with Room Fires, Semi Annual Progress Report, National Science Foundation Grant No. GI 31892 X1, Institute of Technology, Pasadena, CA, 1975.
[48] E.E. Zukoski, in: Proceedings of the First International Symposium on Fire Safety Science, Hemisphere Publishing Corporation, Washington, 1986, pp. 1–30.
[49] P.J. Pagni, Appl. Mech. Rev. (1990) 153–170.
[50] L. Sun, X. Zhou, S. Mahalingam, D.R. Weise, in: Eighth International Symposium on Fire Safety Science, 2005, submitted for publication.